JOURNAL OF THE KOREAN ASTRONOMICAL SOCIETY
37: 299 ~ 305, 2004

IMAGING NON-THERMAL X-RAY EMISSION FROM GALAXY CLUSTERS: RESULTS AND IMPLICATIONS

MARK HENRIKSEN AND DANNY HUDSON
Joint Center for Astrophysics, Physics Department, University of Maryland, Baltimore, MD 21250, USA
E-mail: mark@jca.umbc.edu

ABSTRACT

We find evidence of a hard X-ray excess above the thermal emission in two cool clusters (Abell 1750 and IC 1262) and a soft excess in two hot clusters (Abell 754 and Abell 2163). Our modeling shows that the excess components in Abell 1750, IC 1262, and Abell 2163 are best fit by a steep powerlaw indicative of a significant non-thermal component. In the case of Abell 754, the excess emission is thermal, 1 keV emission. We analyze the dynamical state of each cluster and find evidence of an ongoing or recent merger in all four clusters. In the case of Abell 2163, the detected, steep spectrum, non-thermal X-ray emission is shown to be associated with the weak merger shock seen in the temperature map. However, this shock is not able to produce the flatter spectrum radio halo which we attribute to post-shock turbulence. In Abell 1750 and IC 1262, the shocked gas appears to be spatially correlated with non-thermal emission suggesting cosmic-ray acceleration at the shock front.

Key words : clusters of galaxies – inverse-Compton emission – mergers

I. INTRODUCTION

Inverse-Compton measurements for galaxy clusters have proven problematic using non-imaging detectors to observe the hottest clusters. AGN emission may significantly contaminate the spectra taken of diffuse sources using these detectors (See Section IV). Since radio halo strength has been correlated with cluster X-ray luminosity, the brightest inverse Compton (IC) emission should come from the clusters with the highest temperatures. Thus, the most frequent strategy employed to observe the hard tail of massive clusters has been to use the large field-of-view "light buckets" that extend into the hard X-ray band well beyond the thermal emission (>50 keV) for the hottest clusters.

However, the cluster thermal luminosity increases as T^3 where T is the cluster temperature (Novicki et al. 2003). For inverse Compton emission from cosmic-ray electrons accelerated by merger shocks, the IC emission increases as $T^{1.9}$ (Miniati et al. 2001). Therefore, the ratio of IC emission to thermal emission decreases with temperature. For very hot clusters such as Abell 2163, one must observe above 50 keV. Diffuse non-thermal emission typically has a steep photon spectral index of 2.5 so that the flux at 10 keV is 316 times higher than at 100 keV. Thus, in the energy range above the thermal spectrum of hot clusters, the diffuse non-thermal component will be weaker. AGN, which generally have flatter spectra than the IC emission will then dominate the weak signal of the IC emission. We show that Abell 754 clearly demonstrates this problem.

In addition to the powerlaw giving a higher flux at low energies, the effective area of detectors decreases with energy. For example, the effective area of the BeppoSax PDS (15 - 300 keV) is 10 times lower than the RXTE PCA (2 - 60 Kev). Our approach is to look for non-thermal X-ray emission at low energies using cool clusters or to look for the soft excess signature of hot clusters. For clusters such as Abell 1750 and IC 1262 we can utilize detectors that have imaging (Chandra ACIS) or large effective area, RXTE PCA. For Abell 1750, we have complete imaging of the field-of-view using XMM and ROSAT so that AGN contamination can be accurately modeled. For hot clusters, such as Abell 2163, we use the soft X-ray band of the Chandra ACIS to search for non-thermal emission while using the broad-band detectors to model the thermal emission.

For the hot clusters, such as Abell 2163, AGN contamination will be less of a problem at low energy (< 1 keV) where a steep powerlaw from diffuse emission will dominate both the flat spectrum AGN emission and the thermal component which flattens at low energy. Furthermore, Since soft X-ray spectra can be imaged at high resolution, the NT X-ray emitting region can be isolated as we have done with Chandra for the cool cluster, IC 1262. If cosmic-rays are accelerated at the shock front, then the amount of non-thermal emission relative to thermal is much higher since the shocked gas is relatively localized compared with the bulk of the intracluster medium. Also, the point sources within the region can be identified and removed with imaging data.

II. THE SIGNIFICANCE OF DETECTING INVERSE COMPTON EMISSION

Inverse-Compton studies are important for two reasons: (1) it is a diagnostic of the evolutionary history

Proceedings of The 3rd Korean Astrophysics Workshop on *Cosmic Rays and Magnetic Fields in Large Scale Structure*

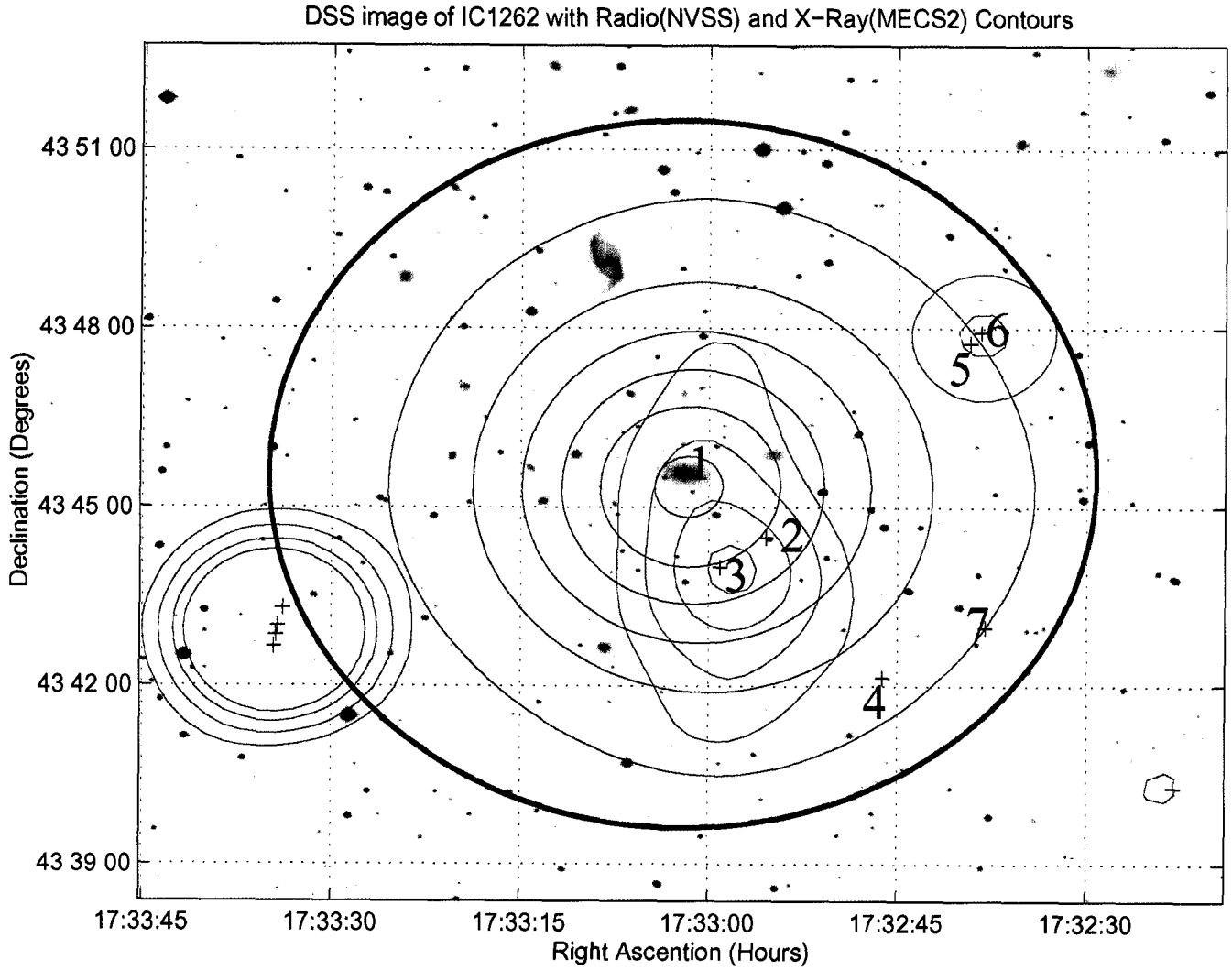

Fig. 1.— Radio (red) and X-ray (blue) contours overlaid on the DSS image The X-ray contours are elongated to the south and show a sloshing morphology in the center. The radio emission shows a N-S radio halo extending 600 kp and having a steep, α 2.7 spectrum.

of a galaxy cluster, and (2) together with diffuse radio maps it can be used to obtain the spatial distribution of the cluster magnetic field. As shown in Henriksen (1998), using the synchrotron flux measured in the radio with the inverse-Compton flux, the magnetic field can be calculated if the spectral index is also well constrained. Thus, by producing maps of non-thermal emission in both radio and X-ray, the magnetic field can be mapped.

The equation of hydrostatic equilibrium, dP/dr = -GM/r, applied to clusters in mass determinations has historically only included gas pressure in the intracluster medium. However, simulations (Miniati et al. 2001) indicate that cosmic-ray protons may contribute up to 40% of gas pressure. If the magnetic field and cosmic-rays are in equipartition then magnetic field support may also be significant. Bulk flow from a recent merger may provide an additional pressure component, though clusters with morphological evidence of a merger can be avoided in mass measurements. Strong lensing cluster mass measurements when compared with X-ray determined mass measurements has implied a missing pressure component in the center of the cluster (Machacek, et al. 2002)

Even without X-ray imaging, the central magnetic field can be calculated from the emission weighted average obtained by a global radio and X-ray flux measurement by making a simple assumption about the radial distribution of the magnetic field. Simulations by Dolag et al. (2002) show that the magnetic fields are frozen into the intracluster medium. Thus the radial profile of the magnetic field can be recovered from the gas density distribution and the emission weighted magnetic field. Using the radio flux map and the B field

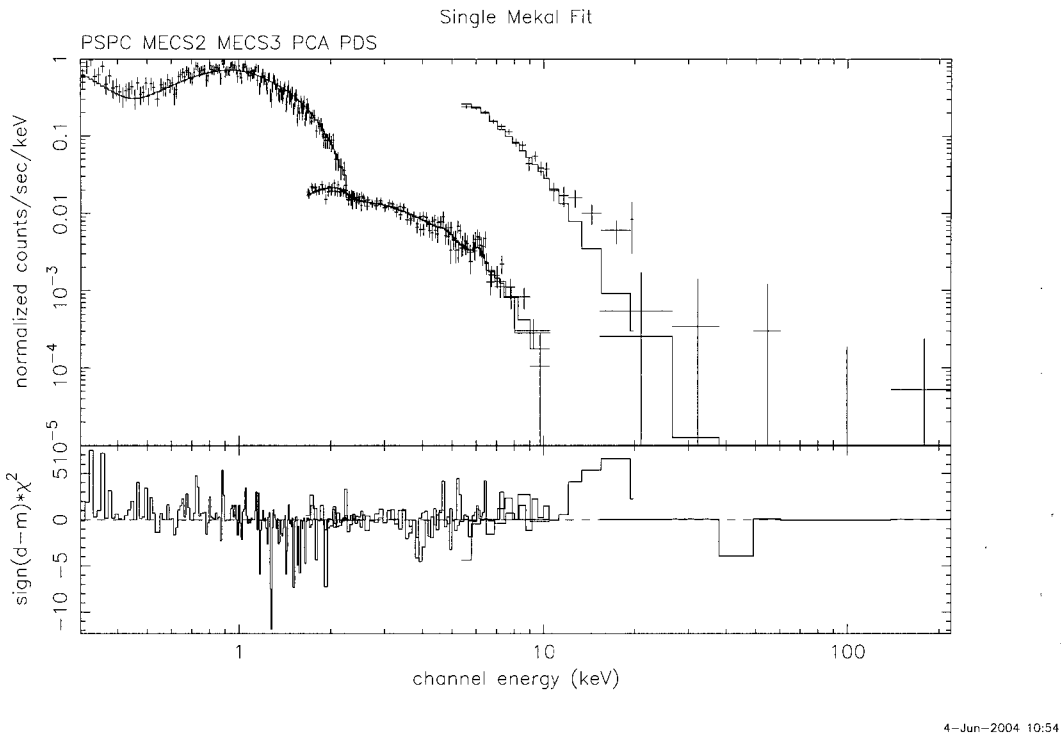

Fig. 2.— Single thermal component fit shows hard, 10 - 20 keV, and soft, < 1 keV, residuals.

radial profile, the cosmic-ray pressure component can then be calculated. The pressure component will be fully determined for the equation of hydrostatic equilibrium and an accurate mass profile can be calculated.

In this paper, we take the first step by presenting our approach to IC measurements and show that merger shocks in galaxy clusters (Abell 2163, IC 1262) and superclusters (Abell 1750) accelerate cosmic-rays. All quantities are quoted with 90% certainty.

III. IC 1262

IC 1262 is a poor group in the Northern Hemisphere at z = 0.034 (Colless et al. 2001). It has a cD galaxy located off center with a very high velocity, 453 km/sec relative to the cluster mean. Cluster cD galaxies in merging systems typically have several hundred km/sec peculiar velocities (Oegerle & Hill 2001). The cD motion is associated with the sloshing that results from an off-center cluster merger (Tittley & Henriksen 2004). The larger velocity of the IC 1262 cD may indicate a recent interaction while the average reflects a range of interaction stages.

Figure 1 shows that there is a diffuse source visible in the NVSS and WENSS data (shown in red). After point source subtraction, there is a visible radio halo extending 600 kpc across with a spectral index estimated from the 1.4 GHz and 330 MHz data of 2.7.

Using Chandra data, we isolated a diffuse non-thermal X-ray component with a photon index of 2.06 - 2.35 and a flux of 7.0 - 10.6$\times 10^{-5}$ photons cm^{-2} s^{-1} at 1 keV that extends from 1.5 - 2.5 arcmin south of the cluster center (Hudson & Henriksen 2003). The non-thermal component is highly localized and co-aligned with the shock front due to the cluster merger as well as overlapping the radio halo. We infer from this spatial relationship that the cosmic-rays have been accelerated by the shock. While the shock appears to be perhaps too weak to give the spectral index, simulations show that stronger merger shocks appear in the center of clusters but accurate Mach numbers are difficult to measure in projection (Ryu et al. 2003)

IV. ABELL 754

Abell 754 has become the prototypical major merger. It is a rich, southern Cluster, B-M type I-II, at a redshift of 0.054. The galaxy distribution shows 2 main clumps: one in the NW and one in the SE with the cD galaxy offset 1.2 arcmin from the NW clump. The X-ray peak is near the SE galaxy clump. Low frequency radio observations (Kassim et al. 2001) show two diffuse features, a relic and a halo straddling the X-ray peak.

Our analysis of the Chandra, BeppoSAX, ASCA, and ROSAT PSPC observations of A754 show evidence of a new soft, diffuse X-ray component (Henriksen, Hudson, & Tittley 2004). The emission extends out to 8' from the X-ray center and is peaked in the cluster center. Fitting a thermal model to the combined BeppoSAX and PSPC spectra show excess emission below 1 keV in the PSPC and above 100 keV in the BeppoSAX

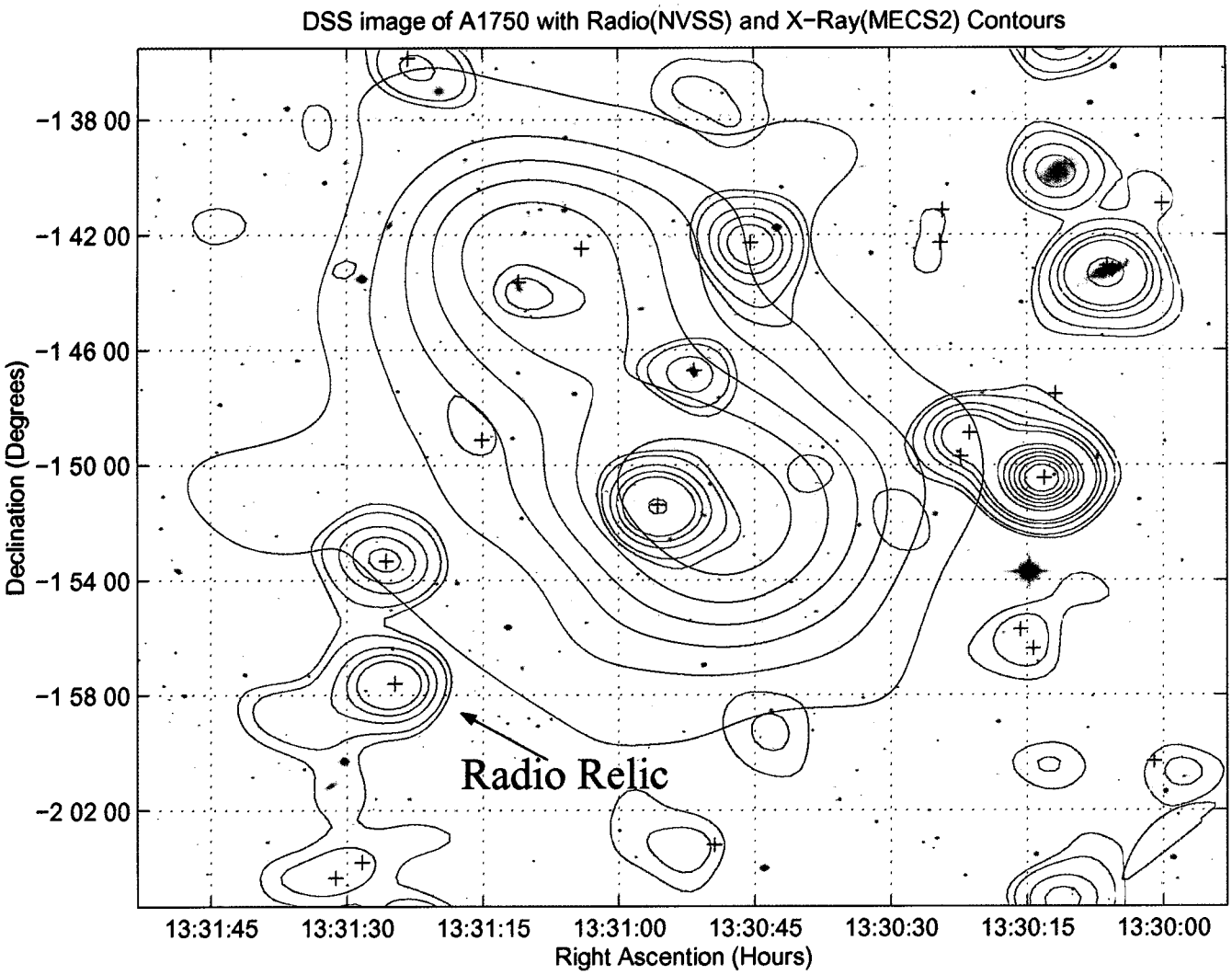

Fig. 3.— BeppoSax MECS X-ray contours are in blue and NVSS radio contours are shown in red overlayed on the DSS map. A radio relic is shown to the East of the main cluster.

PDS. The source, 26W20, is in the field of view of the PDS. The addition of a power law, with the spectral parameters measured by Silverman et al. (1998) for 26W20, successfully models the hard component in the PDS. The excess soft emission can be attributed to a low temperature, 0.77-1.21 keV component. The soft excess is also modeled with a power law, although the 90% uncertainty for the normalization of the power law is consistent with zero. Either component added to a hot thermal component provides a statistically significant improvement over a single hot thermal component. The Chandra temperature map provides a detailed description of the thermal state of the gas on a scale of 100 kpc and larger and does not show any region cooler than 5.9 keV within the region where the cool component was detected. Calculations of the expected emission from one or more groups randomly embedded in a hot gas component were performed that demonstrate that groups are a plausible source of the 1 keV emission, in that they can match the measured cool component luminosity without violating the spatial temperature constraints provided by the temperature map. The cool component gas density and temperature are relatively high, arguing against the warm hot intergalactic medium as the source of the X-ray emission. Furthermore, because the cool component is centrally peaked, the groups are likely embedded in the intracluster gas, rather than in the intercluster gas since this later component is unlikely to show a peak in the cluster center. The typical X-ray emission from early-type galaxies is not high enough to provide the total cool component luminosity, 2.1×10^{43} ergs s^{-1}. The peak of the cool component is located between the low frequency radio halos, thus arguing against a non-thermal interpretation for the emission based on the synchrotron inverse Compton model, which requires that the nonthermal

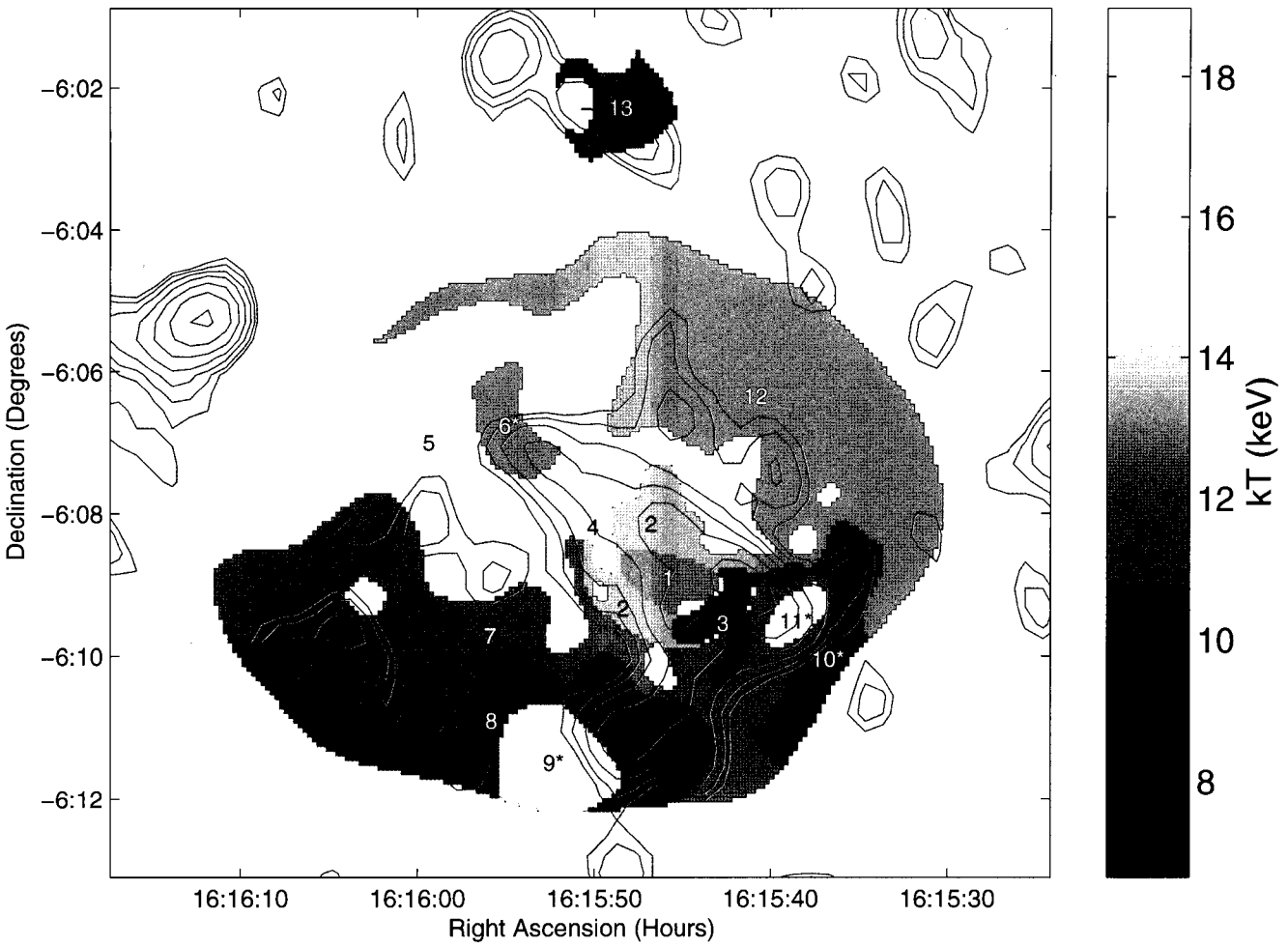

Fig. 4.— Color coded temperature map derived from fitting regions in the Chandra ACIS map of Abell 2163. Overlayed is the NVSS radio contours.

X-ray and radio emission be co-spatial. Thus, we conclude that emission from embedded groups is the most likely origin of the cool component in A754.

V. ABELL 1750

We present evidence for non-thermal emission from the Abell 1750 cluster region. A combined analysis of the RXTE, BeppoSax, and ROSAT spectra for this cluster shows hard residuals of the RXTE PCA in the 1 - 20 keV range (see Figure 2).

This hard excess above the thermal emission in the PCA and below 1 keV in the ROSAT PSPC, is best modeled by a powerlaw. The X-ray photon spectral index for the powerlaw is constrained to better than 5% and ranges from 1.93 - 2.10 with a best fit value of 2.01. Abell 1750 is classified as a bimodal cluster within a supercluster that has had multiple mergers. The cluster itself presently has little shocked gas in the merging atmospheres and is in the very early stage of merger. We found evidence for a radio relic in the NVSS to the East of the main (SW) subcluster (see Figure 3) and suggest that an earlier merger must be responsible for producing the non-thermal X-ray emission. Our conclusion is supported by shocked gas that is visible in the XMM temperature map near the radio relic. This is the first detection of diffuse non-thermal X-ray emission from a merger relic.

VI. ABELL 2163

We report the first detection of diffuse, non-thermal, X-ray emission in an intermediate redshift (z = 0.203) galaxy cluster, Abell 2163. Using *ROSAT-PSPC* and *Chandra-ACIS* data, we found a soft excess, which is best modeled by a steep powerlaw Γ_X = 2.7 - 5.9 with flux of $7.3^{+11.7}_{-5.9} \times 10^{-5}$ photons cm^{-2} s^{-1} keV^{-1} at 1 keV. The X-ray spectral index is consistent with the weak shock ($\mathcal{M}$ = 1.2-1.8) implied by our temperature map. The shocked gas is associated with a cooler, less massive subcluster that has penetrated the main cluster and now lies to the southwest of the main cluster

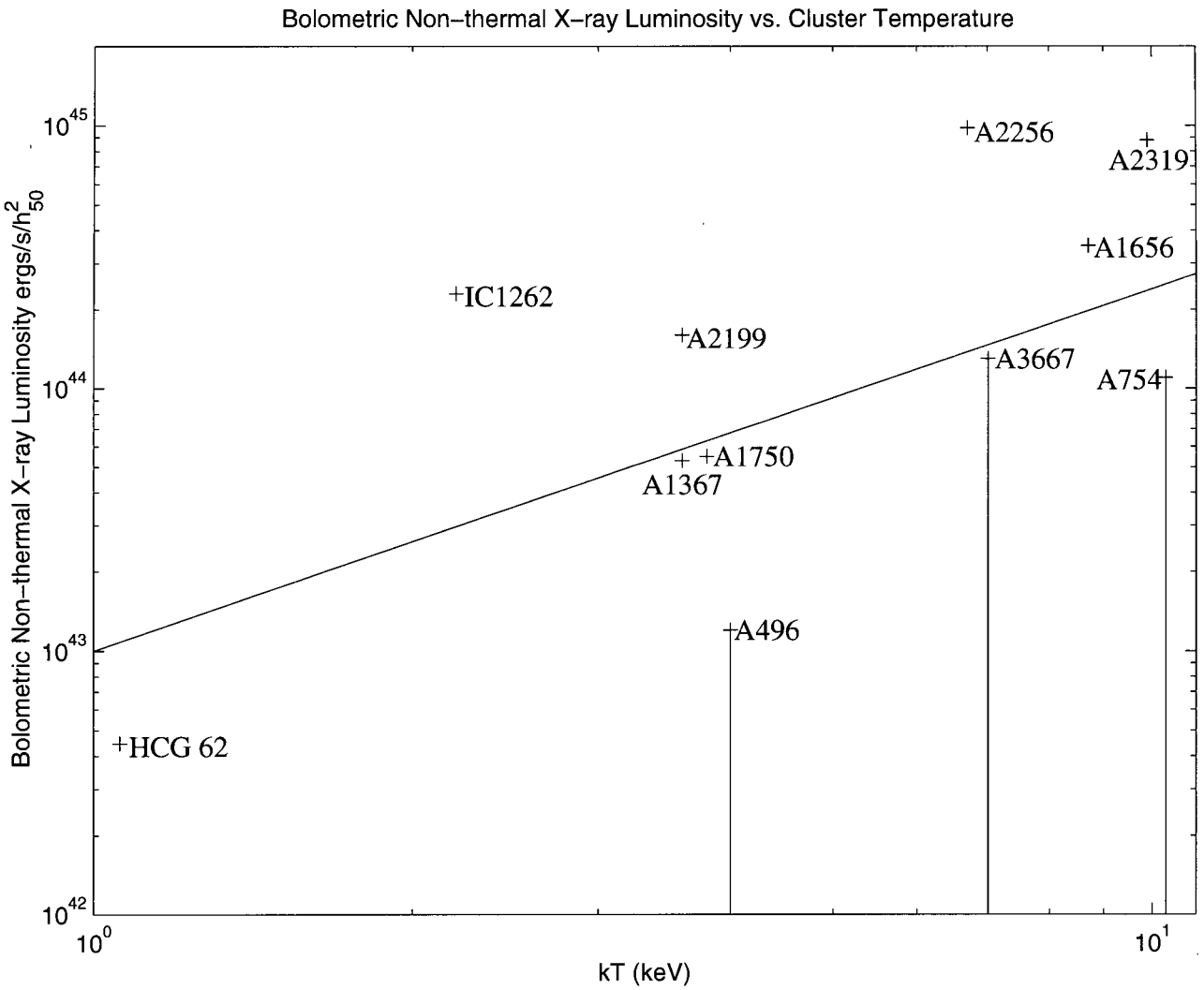

Fig. 5.— The dashed line is predicted for non-thermal X-ray emission produced by primary electrons while the dash-dot line is for secondary. The best fit is more consistent with primary electrons. Secondary electrons overpredict the IC emission for massive clusters. Most striking are A3667 and A754 in which non-thermal emission is not detected in the X-ray though visible in the radio.

core (see Figure 4). By comparing the pressure of cold clump to that of the gas around it, we find that the compression ratio of the shock, $r = 3.1\text{-}4.3$, corresponds to a Mach number of $\mathcal{M} = 1.2\text{-}1.5$. This Mach number is consistent with that inferred from our measured X-ray photon spectral index, using the formalism of Bell (1978). We find that the radio halo, which has a flatter spectral index, would require a much stronger shock, $\mathcal{M} \sim 2.3$. The bremsstrahlung cooling time ($\sim 10^{14}$ yr) of the shocked gas would far exceed the radiative lifetime ($\sim 10^8$) of the radio halo. Thus, it is unlikely that an early, stronger shock produced the radio halo since higher Mach number post-shock gas is not seen in the temperature map. We conclude that the diffuse, non-thermal, X-ray emission originates from the weak merger shock, whereas the radio halo is produced by the turbulence that follows the merger.

VII. L_{nt} VS. TEMPERATURE PLOT

A more powerful shock will produce more cosmic rays. The power of the shock should depend on the velocity of the subcluster collision; a more massive primary cluster should experience a more energetic merger and produce more cosmic rays. Simulations (Miniati et al. 2001) show that the non-thermal luminosity from primary cosmic-rays, those accelerated at the shock front, is proportional to $T_x^{-1.9}$ while the luminosity from secondary electrons depends on the gas density, n_i, and therefore has a steeper proportionality, $T_x^{-3.0}$. Therefore, by measuring the L_{nt} T_x relationship for clusters and groups, one will find a steeper relationship

depending on whether secondary or primary electrons are involved.

Data for Figure 5 was taken from the literature (A1367 - Henriksen & Mushotzky 2001; A2256 - Henriksen 1999; IC 1262 - Hudson & Henriksen 2003; A754 - Henriksen, Hudson & Tittley 2004; A1750 - this paper; A3667 - Rephaeli & Gruber 2004; A2319 - Gruber & Rephaeli 2002; A1656 - Fusco-Femiano et al. 1999; A2199 - Kaastra et al. 1999; A496 - Valinia et al. 2002; HCG 62 - Fukazawa et al., Several things are apparent: (1) there is a correlation which implies that AGN contamination is not likely the dominant source of NT emission in clusters unless more massive clusters are shown to have more or brighter AGN, (2) the fit favors primary cosmic-rays as the source of the non-thermal emission, (3) future work should focus on low temperature clusters and groups since the survey is undersamples at low temperature.

ACKNOWLEDGEMENTS

This work was supported by funding from NASA.

REFERENCES

Bell, A. R., 1978, MNRAS, 182, 147

Colless, M., et al. 2001, MNRAS, 321, 277

Dolag, K., Bartelmann, M., & Lesch, H. 2002, A&A, 387, 383

Fusco-Femiano, R. et al. 1999, ApJ, 513, 21

Fukazawa, et al. 2001, ApJ, 546, 87

Gruber, D., & Rephaeli, Y. 2002, ApJ, 565, 877

Henriksen, M. 1998, PASJ, 50, 389

Henriksen, M. 1999, ApJ, 511, 666

Henriksen, M., Hudson, D., & Tittley, E. 2004, ApJ, 610, 762

Henriksen, M., & Mushotzky, R. 2001, ApJ, 553, 84

Hudson, D., & Henriksen, M. 2003, ApJL, 595, 1

Kaastra, J. 1999, ApJ, 519, 119

Machacek, M., Bautz, M., Canizares, C., & Garmire, G. 2002, ApJ, 567, 188

Miniati, F., Jones, T. W., Kang, H., & Ryu, D. 2001, ApJ, 562, 233

Novicki, M. C., Sornig, M., & Henry, J. P. 2002, AJ, 124, 2413

Oegerle W., & Hill, j. 2001, AJ, 251, 122, 2858

Rephaeli, Y. & Gruber, D. 2004, ApJ, 606, 825

Ryu, D., Kang, H., Hallman, E., & Jones, T. 2003, ApJ, 593, 599

Silverman, J., Harris, D., & Junor, W. 1998, AA, 335, 44

Tittley, E., & Henriksen, M. 2004, ApJ (in press)